*Inorg. Chem.* **2005**, *44*, 1147−1152


# Synthesis and X-ray Crystal Structure of a Cationic Homoleptic $(SPS)_2Rh(III)$ Complex and EPR Study of Its Reduction Process

**Marjolaine Doux,[†] Nicolas Mézailles,[†] Louis Ricard,[†] Pascal Le Floch,*[,†] Prashant Adkine,[‡] Théo Berclaz,[‡] and Michel Geoffroy*[,‡]**

*Laboratoire "Hétéroéléments et Coordination", UMR CNRS 7653, Ecole Polytechnique, 91128 Palaiseau Cédex, France, and Department of Physical Chemistry, 30 quai Ernest Ansermet, University of Geneva, 1211 Geneva, Switzerland*

Received July 19, 2004

Oxidation of the square planar Rh(I) complex $[Rh(SPS^{Me})(PPh_3)]$ ($SPS^{Me}$ = 1-methyl-1-P-2,6-bis(diphenylphosphinosulfide)-3,5-(bisphenyl)-phosphinine) (**1**) based on mixed SPS-pincer ligand with hexachloroethane yielded the Rh(III) dichloride complex $[Rh(SPS^{Me})(PPh_3)Cl_2]$ (**2**), which was structurally characterized. The homoleptic Rh(III) complex $[Rh(SPS^{Me})_2][Cl]$ (**4**) was obtained via the stoichiometric reaction of $SPS^{Me}$ anion (**3**) with $[Rh(tht)_3Cl_3]$ (tht = tetrahydrothiophene). Complex **4**, which was characterized by X-ray diffraction, was also studied by cyclic voltammetry. Complex **4** can be reversibly reduced at $E = -1.16$ V (vs SCE) to give the neutral 19-electron Rh(II) complex $[Rh(SPS^{Me})_2]$ (**5**). Accordingly, complex **5** could be synthesized via chemical reduction of **4** with zinc dust. EPR spectra of complex **5** were obtained after electrochemical or chemical reduction of **4** in THF or $CH_2Cl_2$. Hyperfine interaction with two equivalent $^{31}P$ nuclei was observed in liquid solution, while an additional coupling with a spin $^1/_2$ nucleus, probably $^{103}Rh$, was detected in frozen solution. The $^{31}P$ couplings are consistent with DFT calculations that predict a drastic increase in the axial P–S bond lengths when reducing $(SPS^{Me})_2Rh(III)$. In the reduced complex, the unpaired electron is mainly localized in a rhodium $d_{z^2}$ orbital, consistent with the *g*-anisotropy measured at 100 K.

## Introduction

Multidentate ligands incorporating two or more heteroatoms play an increasing role in coordination chemistry and catalysis. In such systems, steric and electronic properties of the ligands can be finely adjusted to control the stability and reactivity of complexes.[1] Recently, we reported on the synthesis of a new class of mixed SPS ligands featuring a $\lambda^4$-phosphinine unit as central ligand and two ancillary phosphinosulfides groups. These tridentate anionic systems, which are easily assembled from the corresponding phosphinine precursors through the reaction of a nucleophile at the electrophilic atom of phosphinines, readily form very stable complexes with groups 9 and 10 metals.[2,3] Interestingly, square planar Pd(II) complexes were found to be powerful catalysts in the Miyaura cross-coupling process that allows the synthesis of arylboronic esters.[4] In pursuing our investigation, we found that these new ligands can encapsulate metals in two different ways, either acting as a classical tridentate pincer ligand in square planar complexes or capping one face of a trigonal bipyramid. For example, highly reactive 16-electron rhodium (I) species such as **1** (square planar) are able to activate small molecules such as $O_2$, $CS_2$, and $SO_2$ to form the corresponding 18-electron species (trigonal bipyramidal complex) (Scheme 1).

As part of a continuing program aimed at investigating the coordinating behavior of these ligands and the electronic properties of their related complexes, we were led to study the synthesis and the electronic properties of the homoleptic 18-electron Rh(III) species. Herein, we report on these results.

* Authors to whom correspondence should be addressed. E-mail: lefloch@mars.polytechnique.fr (P.L.).
[†] Laboratoire "Hétéroéléments et Coordination".
[‡] University of Geneva.

(1) (a) Albrecht, M.; Van Koten, G. *Angew. Chem., Int. Ed.* **2001**, *40*, 3750−3781. (b) van der Boom, M. E.; Milstein, D. *Chem. Rev.* **2003**, *103*, 1759−1792. (c) Singleton, J. T. *Tetrahedron Lett.* **2003**, *59*, 1837−1857. (d) Braunstein, P.; Naud, F. *Angew. Chem., Int. Ed.* **2001**, *40*, 680−699. (e) Walsh, P. J.; Lurain, A. E.; Balsells, J. *Chem. Rev.* **2003**, *103*, 3297−3344.

(2) Doux, M.; Mézailles, N.; Ricard, L.; Le Floch, P. *Organometallics* **2003**, *22*, 4624−4626.

(3) Doux, M.; Mézailles, N.; Ricard, L.; Le Floch, P. *Eur. J. Inorg. Chem.* **2003**, 3878−3894.

(4) Doux, M.; Mézailles, N.; Melaimi, M.; Ricard, L.; Le Floch, P. *Chem. Commun.* **2002**, 1566−1567.

10.1021/ic049046+ CCC: $30.25 
Published on Web 01/25/2005

**Scheme 1**

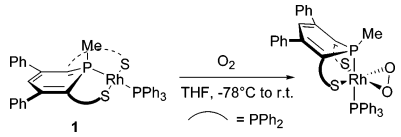


## Results and Discussion

**(i) Syntheses and X-ray Crystal Structures of Complexes 2 and 4.** In a previous study, we showed that complex **1** readily underwent oxidative additions with various reagents to yield Rh(III) species. Supposing that complex **1** could act as a suitable precursor of dihalogeno Rh(III) species, we investigated its oxidation with hexachloroethane. As expected, oxidation of **1** easily takes place in THF at low temperature to afford the 18-electron complex **2** (Scheme 2).

**Scheme 2**

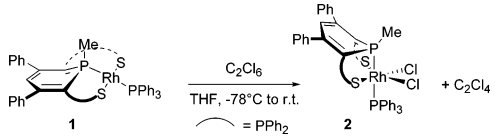


The formulation of **2** could be easily established on the basis of NMR data. As previously observed in related $O_2$ and $CS_2$ complexes, the formation of a Rh(III) complex causes an important deshielding of the P-Me $^{31}$P NMR signal (from $\delta$ (P-Me, THF) = 29.80 in **1** to $\delta$ (P-Me, THF) = 58.17 in **2**). Although all NMR data show that **2** adopts a symmetrical structure, its stereochemistry could not be unambiguously established. Fortunately, suitable microcrystals of **2** could be grown by diffusing hexane into a dichloromethane solution of the complex (see Supporting Information for the X-ray structure of complex **2**). The overall geometry around rhodium is octahedral, and the ligand shapes one side of the octahedron, the central phosphorus ligand lying trans to the triphenylphosphine moiety. As previously noted, only the diastereomer resulting from the syn attack is formed. This facial selectivity has already been rationalized by considering the steric crowding provided by the two axial phenyl groups and the rigidity of the ligand.[2]

Having this complex in hand, we then turned our attention to the synthesis of the homoleptic cationic Rh(III) complex **4**. Unfortunately, reaction of 1 equiv of the anionic ligand **3** with complex **2** only yielded unidentified compounds whose structures could not be established on the sole basis of $^{31}$P NMR data (Scheme 3).

**Scheme 3**

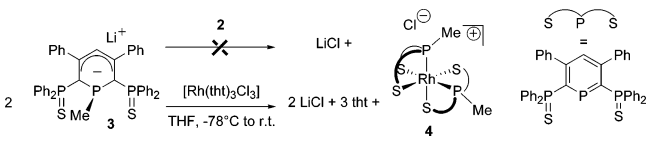


Another alternative to the synthesis of **4** relies on the reaction of 2 equiv of anion **3** with a Rh(III) precursor. Thus, reaction of 2 equiv of **3** with $[Rh(tht)_3Cl_3]$ (tht = tetrahydrothiophene) in THF at low temperature afforded the expected homoleptic complex **4** in good yield (Scheme 3).

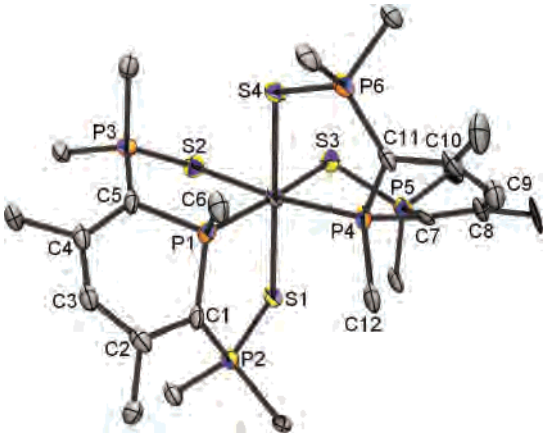


**Figure 1.** ORTEP view of cationic complex **4**. Atoms are drawn as 50% thermal ellipsoids. Phenyl groups have been omitted for clarity.

**Table 1.** Bond Distances (Å) and Bond Angles (deg) for **4**

| | | | |
|---|---|---|---|
| P1−C1 | 1.765(3) | P2−S1 | 2.040(1) |
| C1−C2 | 1.431(4) | P3−S2 | 2.017(1) |
| C2−C3 | 1.392(5) | Rh1−P1 | 2.2661(8) |
| C3−C4 | 1.417(5) | Rh1−P4 | 2.2617(7) |
| C4−C5 | 1.386(4) | Rh1−S1 | 2.3641(8) |
| C5−P1 | 1.806(3) | Rh1−S2 | 2.4462(8) |
| P1−C6 | 1.803(4) | Rh1−S3 | 2.4458(8) |
| C1−P2 | 1.755(3) | Rh1−S4 | 2.3693(8) |
| C5−P3 | 1.781(3) | | |

| | | | |
|---|---|---|---|
| P1−C1−C2 | 114.7(2) | P1−Rh1−S3 | 171.40(3) |
| C1−C2−C3 | 122.3(3) | S1−Rh1−S4 | 178.85(3) |
| C2−C3−C4 | 124.1(3) | P4−Rh1−S2 | 172.06(3) |
| C3−C4−C5 | 122.9(3) | Rh1−S1−P2 | 108.26(4) |
| C4−C5−P1 | 115.9(2) | P1−Rh1−S2−S4 | 91.4 |
| C1−P1−C5 | 101.7(1) | (plane C1−C2−C4−C5)−P1 | 24.2 |
| P1−Rh1−P4 | 98.96(3) | (plane C1−C2−C4−C5)−C3 | 8.5 |
| P1−Rh1−S2 | 88.85(3) | | |
| Σ (angles at *P*1) | | 310.4 | |

After purification, complex **4** was isolated as a very stable orange solid. The stereochemistry of **4** was unambiguously established from the $^{31}$P NMR spectrum that shows the presence of two magnetically nonequivalent diphenylphosphinosulfide groups. Indeed, **4** appears as an $A_2B_2C_2$ spin system that was successfully modeled (see Experimental Section). Suitable crystals of **4** could be obtained by diffusing hexane into a $CDCl_3$ solution of **4**, and an X-ray crystal structure analysis confirmed the proposed stereochemistry. An ORTEP view of cationic complex **4** is presented in Figure 1, and the most significant metric parameters are listed in Table 1. Crystal data and structural refinement details are presented in Table 2. In good agreement with NMR data, the two phosphorus atoms lie in a cis arrangement, leaving two nonequivalent $PPh_2S$ groups. There are many similarities between the structures of **2** and **4**. In both complexes, the Rh−P bonds are quite similar as are internal parameters within the phosphinine ring (dihedral angles between the plane of the ring and the P atom and pyramidality at the phosphorus). The S−Rh bonds fall in the same range in both species, albeit being slightly different in **4** (for example: S4−Rh1 2.3693(8) Å and Rh1−S3 2.4458(8) Å) because of the stereochemistry. So far, no theoretical investigation has been

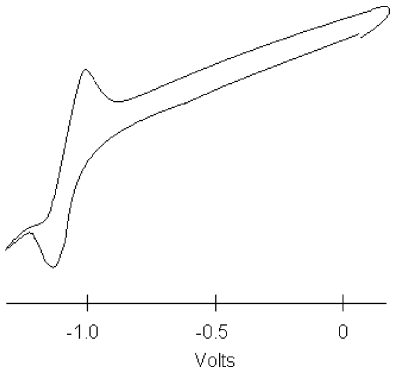


**Figure 2.** Cyclic voltammetric curve (scan rate: 0.05 V $s^{-1}$) of $CH_2Cl_2$ solution (20 °C) containing 2 mM of **4**, 0.3 M of $[NBu_4][BF_4]$ at a gold disc electrode (diameter 0.5 mm).

**Table 2.** Crystal Data and Structural Refinement Details for **4**

| | |
|---|---|
| formula | $C_{84}H_{68}P_6RhS_4$, 6($CHCl_3$), Cl |
| $M_r$ | 2246.01 |
| crystal system | triclinic |
| space group | $P\bar{1}$ |
| $a$[Å] | 16.812(1) |
| $b$[Å] | 17.628(1) |
| $c$[Å] | 20.168(1) |
| α[deg] | 106.398(1) |
| $\beta$[deg] | 93.680(1) |
| $\gamma$[deg] | 117.576(1) |
| $V$[Å$^3$] | 4947.3(5) |
| $Z$ | 2 |
| $\rho$[g cm$^{-3}$] | 1.508 |
| $\mu$(cm$^{-1}$) | 0.911 |
| crystal size [mm$^3$] | 0.22 × 0.22 × 0.14 |
| $F$(000) | 2272 |
| index ranges | $-21 \le h \le 21$; $-22 \le k \le 22$; $-26 \le l \le 26$ |
| scan type | $\varphi$ and $\omega$ scans |
| parameter refined | 975 |
| reflections/parameter | 18 |
| reflections collected | 36627 |
| independent reflections | 22455 |
| reflections used | 17685 |
| wR2 | 0.1706 |
| R1 | 0.0547 |
| goodness of fit | 1.104 |
| largest diff peak/hole [e Å$^{-3}$] | 2.187(0.104)/−1.131(0.104) |

performed to explain why only one diastereoisomer of complex **4** is formed.

**(ii) Electrochemical and Chemical Reduction of Complex 4.** As can be seen in Figure 2, complex **4** can be reversibly reduced at $E^{red} = -1.16$ V (vs SCE) to yield the neutral 19-electron Rh(II) species **5** (scan rate = 0.05 V·s$^{-1}$). Compared to well-known Rh(I) and Rh(III) complexes, only a few mononuclear Rh(II) complexes have been characterized so far.[5−7]

Interestingly, we found that this reduction could be chemically performed using Zn as reducing agent. Thus, reaction of a suspension of **4** in THF at room temperature with Zn dust (in excess) resulted in dissolution of the starting material and a color change from orange to brown. As expected, this reduction is accompanied by the disappearance of the $^{31}$P NMR signal. Complex **5** proved to be stable in solution though highly sensitive toward oxygen. Exposure of a freshly prepared solution of **5** to air resulted in the reformation of complex **4** (Scheme 4). Unfortunately, despite several attempts, no crystals of **5** could be grown. Therefore,

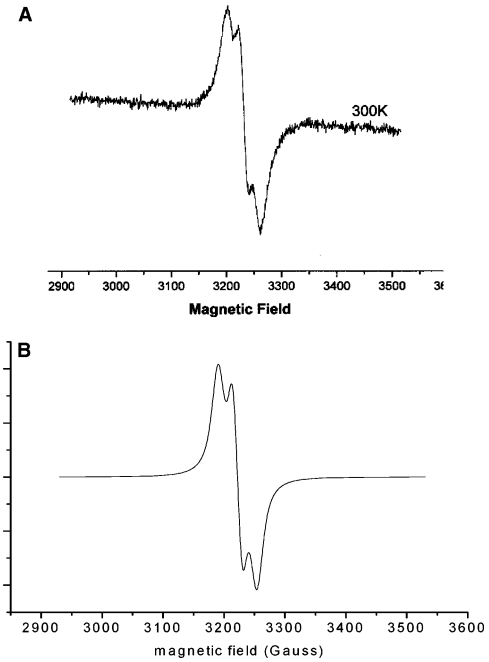


**Figure 3.** (A) EPR spectrum obtained at 300 K after electrochemical reduction of a $CH_2Cl_2$ solution of **4**. (B) Simulated spectrum.

**Scheme 4**

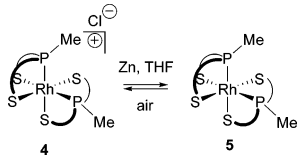


we attempted to get structural information about **5** from its EPR spectra and from DFT calculations.

**(iii) EPR Results.** Electrochemical reduction of a solution of **4**, in situ in the EPR cavity at room temperature, led to the EPR spectrum shown in Figure 3A. This spectrum, centered at $g = 2.0843$, is composed of three broad lines that partly overlap and reflect hyperfine interaction (22.5 G) with two equivalent spin-$^1/_2$ nuclei (two $^{31}$P nuclei). The large line width is probably caused by a rather slow reorientation of this cumbersome complex and by unresolved coupling with additional nuclei ($^{103}$Rh and additional $^{31}$P nuclei). Simulation of this spectrum is given in Figure 3B. Reduction of **4** was also performed chemically. Using sodium naph-

(5) (a) DeWitt, D. G. *Coord. Chem. Rev.* **1996**, *147*, 209−246. (b) Pandey, K. K. *Coord. Chem. Rev.* **1992**, *121*, 1−42. (c) Shaw, M. J.; Geiger, W. E.; Hyde, J.; White, C. *Organometallics* **1998**, *17*, 5486-5494. (d) Garcia, M. P.; Jimenez, M. V.; Lahoz, F. J.; Lopez, J. A.; Oro, L. A. *J. Chem. Soc., Dalton Trans.* **1998**, 4211−4214. (e) Paul, P.; Tyagi, B.; Bilakhiya, A. K.; Bhadbhade, M. M.; Suresh, E. *J. Chem. Soc., Dalton Trans.* **1999**, 2009−2014. (f) Connelly, N. G.; Emslie, D. J. H.; Geiger, W. E.; Hayward, O. D.; Linehan, E. B.; Orpen, A. G.; Quayle, M. J.; Rieger, P. H. *J. Chem. Soc., Dalton Trans.* **2001**, 670−683. (g) Willems, S. T. H.; Russcher, J. C.; Budzelar, P. H. M.; de Bruin, B.; de Gelder, R.; Smits, J. M. M.; Gal, A. W. *Chem. Commun.* **2002**, 148−149. (h) Dixon, F. M.; Masar, M. S., III; Doan, P. E.; Farrell, J. R.; Arnold., F. P., Jr.; Mirkin, C. A.; Incarvito, C. D.; Zakharov, L. N.; Rheingold, A. L. *Inorg. Chem.* **2003**, *42*, 3245−3255. (i) Hetterscheid, D. G. H.; Smits, J. M. M.; de Bruin, B. *Organometallics* **2004**, *23*, 4236−4246.
(6) Gerisch, M.; Krumper, J. R.; Bergman, R. G.; Tilley, D. T. *Organometallics* **2003**, *22*, 47−58.
(7) Kaim, W.; Rheinhardt, R.; Greulich, S. *Organometallics* **2003**, *22*, 2240−2244.

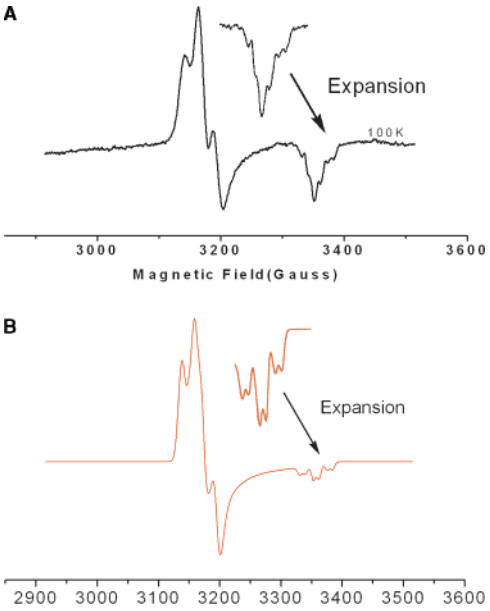


**Figure 4.** (A) EPR spectrum obtained at 100 K after reduction of a solution of a THF solution of **4** with sodium naphthalenide. (B) Simulated spectrum.

thalenide, potassium mirror, or Zn dust at room temperature as a reducing agent leads to intense spectra very similar to the spectrum shown in Figure 3A.[8]

Moreover, as shown in Figure 4A, clear frozen solution spectra could be recorded at 100 K after chemical reduction. Such a spectrum exhibits an intense triplet at $\mathbf{g} = 2.1197$, and a more complicated pattern appears around $g = 1.999$. The shape of the spectrum indicates an axial $g$ tensor. Moreover, the coupling with two spin-$^1/_2$ nuclei measured on the "perpendicular" component is close to the coupling measured on the isotropic spectrum; this implies that the "parallel" hyperfine components for the corresponding nuclei are also close to 22 G. Taking these $g$ and hyperfine properties into account, the simulation of the "parallel" set implies the contribution of an additional spin-$^1/_2$ nucleus (Figure 4B).[9] The corresponding splitting, close to 9 G, is attributed to $^{103}$Rh (natural abundance 100%), while the two equivalent hyperfine constants (22.5 G) are attributed to $^{31}$P nuclei.

The $g_{average}$ value is appreciably different from that of the free electron and indicates that a metal is likely to participate in the structure of the detected paramagnetic species. It is well established that mononuclear $d^7$ complexes of platinum metals adopt a low spin configuration.[10] Because of the Jahn−Teller effect, the octahedral complexes in the $(t_{2g})^6(e_g)^1$ configuration undergo an axial distortion with the unpaired electron in a $d_{z^2}$ ($g_\perp > g_{||}$) or a $d_{x^2-y^2}$ ($g_\perp < g_{||}$) orbital. The spectrum of Figure 4A, with $g_\perp \geq g_{||}$, is consistent with a Rh(II) ion in an octahedral environment with tetragonal elongation. These results, together with the reversible one-electron reduction wave observed by cyclic voltammetry, indicate that the spectra shown in Figures 3 and 4 can be attributed to **5**.

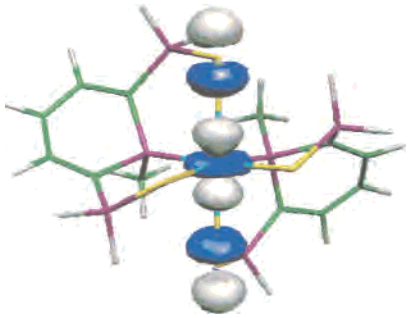

**Figure 5.** Representation of the SOMO of **5′**.

**Table 3.** Bond Distances (Å) and Bond Angles (deg) for **4′** and **5′**

| | **4′ DFT** | **5′ DFT** |
|---|---|---|
| | Bond Distances (Å) | |
| Rh−S4 | 2.458 | 2.937 |
| Rh−S1 | 2.458 | 2.937 |
| Rh−S2 | 2.536 | 2.534 |
| Rh−S3 | 2.536 | 2.534 |
| Rh−P1 | 2.350 | 2.343 |
| Rh−P4 | 2.350 | 2.343 |
| | Bond Angles (deg) | |
| P1−Rh−P4 | 100.5 | 99.09 |
| S1−Rh−S4 | 176.0 | 175.3 |
| Rh−S1−P2 | 103.0 | 96.0 |

**(iv) DFT Calculations.** To confirm this identification, we tried to optimize the geometries of **4** and **5** by using DFT calculations. However, because of the large size of the complex, calculations were performed on model complexes **4′** and **5′** in which the phenyl rings are replaced by hydrogen atoms. As shown in Table 3, the resulting structure, calculated in the $C_2$ symmetry, clearly shows a drastic elongation of the "axial" S−Rh bonds, going from **4′** to **5′**. As shown by the ligand field theory[11] for a mixed-ligand complex, $[ML_4X_2]$, the stabilized structure depends on the relative $\sigma$-bonding strength of the ligands. When X is a slightly more $\sigma$-donor ligand than L, the resulting geometry is expected to exhibit rather short bonds to X and intermediate and long bonds to L; this is in good accordance with the optimized structure of **5′**. For such a system with two elongated Rh−L bonds, the **g** tensor is expected to be axial with $g_\perp > g_{||}$ as found for **5** ($g_\perp = 2.1197$, $g_{||} = 1.999$).

The calculated isotropic $^{31}$P couplings are in reasonable agreement with the EPR spectra; while the hyperfine constants of the two phosphorus atoms (P1 and P4) bound to the rhodium atom are close to 8 G, the interactions with the other $^{31}$P nuclei are ≤3 G (P2, P6: $A_{iso} = 3$ G; P3, P5: $A_{iso} = -0.5$ G) and will likely only contribute to a broadening of the lines. Consistent with the frozen solution spectra, the dipolar interaction is small for all $^{31}$P nuclei. As shown in Figure 5, the unpaired electron is mainly localized in a molecular orbital formed by the rhodium $d_{z^2}$ orbital and a p orbital of each sulfur atom in axial position. From the SOMO coefficients, the spin density on each sulfur atom is equal to 0.21 in the axial position and to 0.02 in the equatorial

(8) Chemical reductions lead to $A_{iso}$ values equal to 21.5 G and to $g$ values equal to 2.0843 (Zn), 2.0850 (Na naphthalenide), and 2.0854 (K mirror).
(9) The optimized frozen solution spectrum, calculated with the program mentioned in ref 16, is given as Supporting Information.
(10) Pandey, K. K. *Coord. Chem. Rev.* **1992**, *121*, 1−42.
(11) Figgis, B. N.; Hitchman, M. In *Ligand Field Theory and its Applications*; Wiley-VCH: New York, 2000.

position. The spin delocalization on each heterocycle is rather small $\rho \approx 0.07$ (with a contribution $\rho = 0.045$ from the phosphorus atom). The Rh coupling is not resolved on the liquid-phase EPR spectrum, but as shown in Figure 4B, it participates in the structure of the parallel component of the frozen solution spectrum.[12]

The present EPR results are consistent with the spectra reported by Dunbar et al. for $[Rh(TMPP)_2][BF_4]_2$ (TMPP = tris(2,4,6-tri-methoxypheny1)phosphine),[13] one of the rare crystallized hexacoordinated Rh(II) monomers; both **g** tensors are axial with $g_\perp > g_{||}$ and a $^{103}$Rh hyperfine splitting is detected. Nevertheless, the $^{31}$P couplings observed for **5**, as well as its smaller *g* anisotropy, suggest that the spin delocalization on the ligands is slightly larger for **5** than for $[Rh(TMPP)_2][BF_4]_2$. As expected, the EPR parameters are drastically dependent upon the structure of the complex. It was shown that in four-coordinated Rh(II) compounds (e.g., $[RhXY(PCy_3)_2]$ with X,Y: halogen, Cy: cyclohexyl), the ground state corresponds to a mixture of $d_{z^2}$ and $d_{xz}$, leading to a very large anisotropy of the **g** tensor.[14] In the same context, Rh(II) complexes of pincer ligands[6] exhibit a **g** tensor that is not axial ($g_1 = 2.864$, $g_2 = 2.320$, $g_3 = 1.9041$). A rhombic *g* tensor was also recently reported for the Rh-(II) complex obtained after long-time reduction of $[(C_6Me_5)$-Rh(abpy)Cl][Cl] (abpy = 2,2′-azobis-pyridine).[7]

## Experimental Section

**General Remarks.** All reactions were routinely performed under an inert atmosphere of argon or nitrogen by using Schlenk and glovebox techniques and dry deoxygenated solvents. Dry THF and hexanes were obtained by distillation from Na/benzophenone and dry ether from $CaCl_2$ and then NaH and dry $CH_2Cl_2$ from $P_2O_5$. $CDCl_3$ was dried from $P_2O_5$ and stored on 4 Å Linde molecular sieves. Nuclear magnetic resonance spectra were recorded on a Bruker 300 Advance spectrometer operating at 300.0 MHz for $^1$H, 75.5 MHz for $^{13}$C, and 121.5 MHz for $^{31}$P. Solvent peaks are used as internal references relative to $Me_4Si$ for $^1$H and $^{13}$C chemical shifts (ppm); $^{31}$P chemical shifts are relative to an 85% $H_3PO_4$ external reference. Coupling constants are given in hertz. The following abbreviations are used: s, singlet; d, doublet; t, triplet; q, quadruplet; p, pentuplet; m, multiplet; v, virtual. The numbering of atoms is the same as the numbering of the structure. Elemental analyses were performed by the "Service d'Analyse du CNRS", at Gif sur Yvette, France. Complex **1**,[2] anion **3**,[3] and $[Rh(tht)_3Cl_3]$[15] were prepared according to reported procedures.

**Synthesis of Complex 2.** Hexachloroethane (21 mg, 0.09 mmol) was added to a solution of **1** (100 mg, 0.09 mmol) in THF (4 mL) at −78 °C. The solution was warmed to room temperature and stirred for 1 h, during which it turned from brown to orange. The solvent was evaporated, and the solid was washed with ether (2 mL) and hexanes (4 mL). **2** was recovered as an orange solid. Suitable crystals for X-ray structure analysis were grown by diffusion of hexanes into a solution of $CH_2Cl_2$. Yield: 85%, 87 mg. $^1$H ($CD_2Cl_2$): $\delta$ 2.28 (dd, $^2J$ (H−P$_1$) = 12.3, $^3J$ (H−Rh) = 3.0, 3H, $CH_3$), 5.93 (t, $^4J$ (H−P$_{2,3}$) = 4.0, 1H, $H_3$), 6.76−7.98 (m, 45H, and H of $C_6H_5$). $^{13}$C ($CD_2Cl_2$): $\delta$ 9.5 (d, $^1J$ (C−P$_1$) = 48.5, $CH_3$), 70.8 (m, $C_{1,5}$), 119.6 (vq, $^3J$ (C−P$_1$) = $^3J$ (C−P$_{2,3}$) = 11.3, $C_3$), 127.3−131.9 (m, CH, and C of $C_6H_5$), 132.3 (dd, $^1J$ (C−P) = 33.2, $^3J$ (C−P) = 3.8, C of $C_6H_5$), 132.6−132.8 (m, CH, and C of $C_6H_5$), 133.4 (dd, $^1J$ (C−P) = 112.5, $^3J$ (C−P) = 11.3, C of $C_6H_5$), 134.1−135.3 (m, CH, and C of $C_6H_5$), 142.2 (m, $C_{2,4}$), 155.8 (bs, C of $C_6H_5$). $^{31}$P ($CD_2Cl_2$): $\delta$ 8.71 ($AB_2CM$, ddt, $^2J$ (P$_4$−P$_1$) = 515.5, $^1J$ (P−Rh) = 82.62, $^3J$ (P$_4$−P$_{2,3}$) = 34.0, $P_4Ph_3$), 52.27 ($AB_2C$, $^2J$ (P$_{2,3}$−P$_1$) = 42.3, $^3J$ (P$_{2,3}$−P$_4$) = 34.0, $P_{2,3}Ph_2$), 58.68 ($AB_2CM$, ddt, $^2J$ (P$_1$−P$_4$) = 515.5, $^2J$ (P$_1$−P$_{2,3}$) = 106.7, $^2J$ (P$_1$−Rh) = 102.2, $P_1$Me). $C_{60}H_{49}Cl_2P_4RhS_2$ (1131.9): calcd C 63.67, H 4.36; found C 63.14, H 3.89.

**Synthesis of Complex 4.** $[Rh(tht)_3Cl_3]$ (334 mg, 0.22 mmol) was added to a red solution of **2** (310 mg, 0.44 mmol) in THF (15 mL) at −78 °C. The solution was warmed to room temperature, stirred for 48 h, and became orange. After removing the solvent, the resulting solid was dissolved in $CH_2Cl_2$ (20 mL) and filtered through Celite. After evaporating the solvent under vacuum, the solid was washed several times with hexanes (3 × 5 mL) and ether (3 × 5 mL). After drying, **4** was recovered as an orange solid. Suitable crystals for X-ray structure analysis were grown by diffusion of hexanes into a solution of $CHCl_3$. Yield: 87%, 280 mg. $^1$H NMR ($CDCl_3$): $\delta$ 1.72 (d, $^2J$ (H−P$_1$) = 10.3, 6H, $CH_3$), 5.89 (t, $^4J$ (H−P$_{2,3}$) = 3.3, 2H, $H_3$), 6.70−7.93 (m, 60H, CH of $C_6H_5$). $^{13}$C NMR ($CDCl_3$): $\delta$ 15.4 (m, $\Sigma J$ = 66.0, $CH_3$), 63.8 (m, $C_{1\text{ or }5}$), 80.7 (m, $C_{5\text{ or }1}$), 123.3 (virtual t, $J$ (C−P$_{2,3}$) = 11.3, $C_3$H), 127.7−134.3 (m, CH, and C of $C_6H_5$), 140.7 (m, $\Sigma J$ = 23.0, C of $C_{2\text{ or }4}$), 140.9 (m, $\Sigma J$ = 23.0, C of $C_{4\text{ or }2}$), 155.9 (m, $\Sigma J$ = 10.0, C of $C_6H_5$), 156.8 (m, $\Sigma J$ = 9.0, C of $C_6H_5$). $^{31}$P NMR ($CDCl_3$): $\delta$ 45.80 ($A_2B_2C_2$, d, $^2J$ (P$_2$−P$_1$) = 72.9, $P_2Ph_2$), 51.75 ($A_2B_2C_2$, d, $^2J$ (P$_3$−P$_1$) = 93.0, $P_3Ph_2$), 57.62 ($A_2B_2C_2$, virtual q, $^1J$ (P$_1$−Rh) = 105.0, $^2J$ (P$_1$−P$_3$) = 93.0, $^2J$ (P$_1$−P$_2$) = 72.9, $P_1$Me). $C_{84}H_{68}$-$ClP_6RhS_4$ (1529.9): calcd C 65.95, H 4.48; found C 65.51, H 4.07.

**Synthesis of Complex 5.** Reduction of **4** (100 mg, 0.07 mmol) was carried out in THF (10 mL) with zinc in excess (100 mg, 1.5 mmol). The solution was stirred for 12 h in the glovebox, and the solvent was evaporated. A change of color from orange to brown was observed. Toluene (5 mL) was added, and the solution was filtered. After evaporation of the solvent, complex **5** was recovered as a brown powder. Yield: 95%, 91 mg. $C_{84}H_{68}P_6RhS_4$ (1497.2): calcd C 67.51, H 4.59; found C 67.22, H 4.30

**Electrochemical Study of Complex 4.** The cyclic voltammetry of **4** (2 mM) in $CH_2Cl_2$ containing [*n*-Bu$_4$N][BF$_4$] (0.3 M) was performed at a stationary gold-disk electrode at room temperature. Transient cyclic voltammetry was performed in a 12 mL three-electrode airtight cell connected to a Schlenck line. The working electrode consisted of a gold disk of 0.5 or 0.125 mm diameter made of a cross section of a gold wire (Goodfellow) sealed in glass. The reference electrode was an SCE (Tacussel), separated from the solution by a bridge (3 mL) filled with a 0.3 M solution of *n*-Bu$_4$BF$_4$ in $CH_2Cl_2$ identical to that used in the cell. The counter electrode was a platinum spiral of ∼1 cm$^2$ apparent surface located within 5 mm of the working electrode and facing it. An Electrochemical Digital Analyzer DEA-I (Radiometer Coppenhagen), which includes a DEA 332 potentiostat equipped with a positive feedback for ohmic drop compensation, was used for experiments.

(12) From these DFT values, ∼70% of the spin is delocalized on the ligands. Using effective core potential is not appropriate for calculation of $^{103}$-Rh couplings. Nevertheless, comparing the experimental $^{103}$Rh isotropic ($A_{iso} \approx 0$ G) and anisotropic ($\tau_{||} = 9$ G) with the atomic coupling constants [Morton, J. R.; Preston, J. *J. Magn. Reson.* **1978**, *30*, 577] leads to a rough estimation of the Rh spin density, $\rho \approx 0.36$, which reasonably agrees with the DFT results.

(13) (a) Dunbar, K. R.; Haefner, S. C. *Organometallics* **1992**, *11*, 1431−1433. (b) Dunbar, K. R.; Haefner, S. C.; Pence, L. E. *J. Am. Chem. Soc.* **1989**, *111*, 5504−5506.

(14) Van Gaal, H. L. M.; Verlaak, J. M. J.; Posno, T. *Inorg. Chim. Acta* **1977**, *23*, 43−51.

(15) Allen, E. A.; Wilkinson, W. *J. Chem. Soc., Dalton Trans.* **1972**, 613−617.

**EPR Spectroscopy.** EPR spectra were recorded on a Bruker 200 and a Bruker ESP 300 spectrometer (X-band) equipped with a variable-temperature attachment. THF was freshly distilled from Na and $CH_2Cl_2$ from $P_2O_5$. Solutions were degassed by several freeze−pump−thaw cycles. Electrochemical reduction was performed, in situ, in the EPR cavity by using an electrolytic cell equipped with platinum electrodes and a EGG PAR 362 potentiostat. Tetrabutylammoniumhexafluorophosphate was used as the electrolyte. Optimization and simulation of the frozen solution spectra were performed with a program based on the Levenberg−Marquardt algorithm.[16]

**DFT Calculations.** DFT calculations were carried out with the Gaussian98 and Gaussian03[17] packages using B3LYP functional.[18] The 6-31G* basis set was used for the ligand atoms, and LANL2DZ was used for rhodium. Optimization of both the **4′** and **5′** complexes were performed assuming $C_2$ symmetry. The SOMO was represented with the MOLEKEL program.[19]

**X-ray Crystallographic Study.** Data were collected at 150.0(1) K on a Nonius Kappa CCD diffractometer using a Mo Kα ($\lambda = 0.71070$ Å) X-ray source and a graphite monochromator. All data were measured using $\varphi$ and $\omega$ scans. Experimental details are described in Table 2. The crystal structures were solved using SIR97[20] and SHELXL-97.[21] ORTEP drawings were made using ORTEP III for Windows.[22] CCDC-261336 and -261337 contain the supplementary crystallographic data for this paper. These data can be obtained free of charge at www.ccdc.cam.ac.uk/conts/retrieving.html [or from the Cambridge Crystallographic Data Centre, 12, Union Road, Cambridge CB2 1EZ, UK; fax: (international) +44-1223/336-033; E-mail: deposit@ccdc.cam.ac.uk].

**Acknowledgment.** We thank the CNRS, the DGA, the Ecole Polytechnique, and the Swiss National Science Foundation for support of this research.

**Supporting Information Available:** ORTEP view of complex **2**, tables of X-ray data, positional and thermal parameters, and bond lengths and angles for complexes **2** and **4**; simulation of the liquid-phase EPR spectrum obtained after reduction of **4**; simulation of the frozen solution EPR spectrum obtained after reduction of a solution of **4** with sodium naphthalenide; fully labeled optimized geometries, standard orientation, energies, and frequencies of **4′** and **5′**; X-ray crystallographic data in CIF format. This material is available free of charge via the Internet at http://pubs.acs.org.

IC049046+

(16) Soulié, E.; Berclaz, T.; Geoffroy, M. In *Computer and Chemistry*, AIP Conference Proceedings 330, Nancy, France, May 1994; Bernardi, F., Rivail, J.-L., Eds.; 1996; pp 627−628.

(17) Frisch, M. J.; Trucks, G. W.; Schlegel, H. B.; Scuseria, G. E.; Robb, M. A.; Cheeseman, J. R.; Zakrzewski, V. G.; Montgomery, J. A., Jr.; Stratmann, R. E.; Burant, J. C.; Dapprich, S.; Millam, J. M.; Daniels, A. D.; Kudin, K. N.; Strain, M. C.; Farkas, O.; Tomasi, J.; Barone, V.; Cossi, M.; Cammi, R.; Mennucci, B.; Pomelli, C.; Adamo, C.; Clifford, S.; Ochterski, J.; Petersson, G. A.; Ayala, P. Y.; Cui, Q.; Morokuma, K.; Malick, D. K.; Rabuck, A. D.; Raghavachari, K.; Foresman, J. B.; Cioslowski, J.; Ortiz, J. V.; Stefanov, B. B.; Liu, G.; Liashenko, A.; Piskorz, P.; Komaromi, I.; Gomperts, R.; Martin, R. L.; Fox, D. J.; Keith, T.; Al-Laham, M. A.; Peng, C. Y.; Nanayakkara, A.; Gonzalez, C.; Challacombe, M.; Gill, P. M. W.; Johnson, B. G.; Chen, W.; Wong, M. W.; Andres, J. L.; Head-Gordon, M.; Replogle, E. S.; Pople, J. A. *Gaussian 98*; Gaussian, Inc.: Pittsburgh, PA, 1998.

(18) (a) Stephens, P. J.; Delvin, F. J.; Chabalowski, C. F.; Frisch, M. J. *J. Phys. Chem.* **1994**, *98*, 11623−11627. (b) Lee, C.; Yang, W.; Parr, R. G. *Phys. Rev. B* **1988**, *B 37*, 785−789.

(19) Flukiger, P. Development of Molecular Graphics Package *MOLEKEL*. Ph.D. Thesis, University of Geneva, Geneva, Switzerland, 1992.

(20) Altomare, A.; Burla, M. C.; Camalli, M.; Cascarano, G.; Giacovazzo, C.; Guagliardi, A.; Moliterni, A. G. G.; Polidori, G.; Spagna, R. *SIR97*, an integrated package of computer programs for the solution and refinement of crystal structures using single-crystal data.

(21) Sheldrick, G. M. *SHELXL-97*; Universität Göttingen: Göttingen, Germany, 1997.

(22) Farrugia, L. J. *ORTEP-3*; Department of Chemistry, University of Glasgow: Glasgow, current release 2003.